Brief Report

Exploring differences for motor imagery using Teager energy operator-based EEG microstate analyses

Yabing Li[1,2,*], Mo Chen[1], Shujun Sun[1], Zipeng Huang[1]

[1] School of Computer Science and Technology, Xi'an University of Posts and Telecommunications, 710121 Xi'an, Shaanxi, China

[2] Shaanxi Key Laboratory of Network Data Analysis and Intelligent Processing, 710121 Xi'an, Shaanxi, China

*Correspondence: liyabing@xupt.edu.cn (Yabing Li)

DOI:10.31083/j.jin2002042

This is an open access article under the CC BY 4.0 license (https://creativecommons.org/licenses/by/4.0/).

Submitted: 21 December 2020 Revised: 3 February 2021 Accepted: 2 March 2021 Published: 30 June 2021

In this paper, the differences between two motor imagery tasks are captured through microstate parameters (occurrence, duration and coverage, and mean spatial correlation (Mspatcorr)) derived from a novel method based on electroencephalogram microstate and Teager energy operator. The results show that the significance between microstate parameters for two tasks is different ($P < 0.05$) with paired t-test. Furthermore, these microstate parameters are utilized as features. Support vector machine is utilized to classify the two tasks with a mean accuracy of 93.93%, which yielded superior performance compared to the other methods.

Keywords

Motor imagery; Microstate parameters; Teager energy operator; EEG signals; Classifier

1. Introduction

Neurophysiological research of activation areas in the brain's sensorimotor cortex plays a crucial role in understanding of motor imagery [1, 2]. This research field can provide relevant information about brain network dynamics and has driven tremendous neuroimaging techniques [3]. Information regarding the brain at high space and time resolution obtained from non-invasive imaging techniques (such as functional magnetic resonance imaging (fMRI) [4], magnetoencephalogram (MEG) [5], positron emission tomography (PET) [6], electroencephalogram (EEG) [7]) can further help in understanding event-related processing in the brain [8].

Electroencephalogram is one of the most widely utilized methods. Despite its limitations regarding spatial resolution, it is relatively easy to obtain and can convey information about the underlying functional brain networks by extracting the relevant information [9]. Several attempts have been made to explore the dynamics of EEG signals for different motor imagery. As one of several procedures developed to undertake motor imagery classification, many researchers focus on feature extraction methods. In recent researchers, time-frequency-based feature extraction methods have been proposed, such as power spectrum density [10, 11], empirical mode decomposition (EMD) [12], and spectral features [13]. However, these methods have the disadvantage of lacking spatial information. Considering that the common spatial pattern (CSP) from EEG signals and its improved algorithm contains the spatial information, they have been widely used, for example, traditional CSP [14], FBCSP [15], complete information common spatial pattern (CICSP) [16] etc. Apart from CSP and its improved algorithm, other methods may also contain spatial information, such as graph theory [17], phase lock value (PLV) [18] and partial directed coherence (PDC) [19]. This paper investigates and compares the proposed method with other researchers who have used the same database.

Selecting practical features plays a vital role in a sound motor imagery classification system. Considering that EEG signals in different brain regions are significantly correlated with left and right movement imaging [18], microstates are exploited to measure quasi-stable scalp voltage configurations [20, 21]. Lehmann proved that the specific frequency band (8–12 Hz) of the EEG signals could be converted into discrete states, which are called "microstates", are defined by topographies of electric potentials recorded over the scalp, and that they can remain stable for 80–120 ms before rapidly transitioning to a different microstate [22, 23]. Some recent articles also provided a critical view of the topography at any given time point is in one state and emphasized the continuous nature of the EEG dynamics that underlie microstate sequences [24, 25]. So microstates obtained from EEG signals can be used in brain-computer interface systems (BCIs) to control external devices (e.g., robotic arms [26], intelligent wheelchairs [27] and other external equipment [28]).

EEG microstates provide a relatively simple but effective methodology for functional description of the global brain network and neural dynamics [29, 30]. We hypothesized that microstates represent the building blocks of imagery and that the way for microstate to analyze the motor imagery tasks-related behavior of EEG is through the changing of frequency and amplitude represented global field power (GFP). However, few researchers have investigated an improved method for the extraction of microstate parameters. Accordingly, we proposed a new framework combining microstate and Teager energy operator (MIC-TEO) for motor imagery task detection.

©2021 The Author(s). Published by IMR Press.

Journal of Integrative Neuroscience

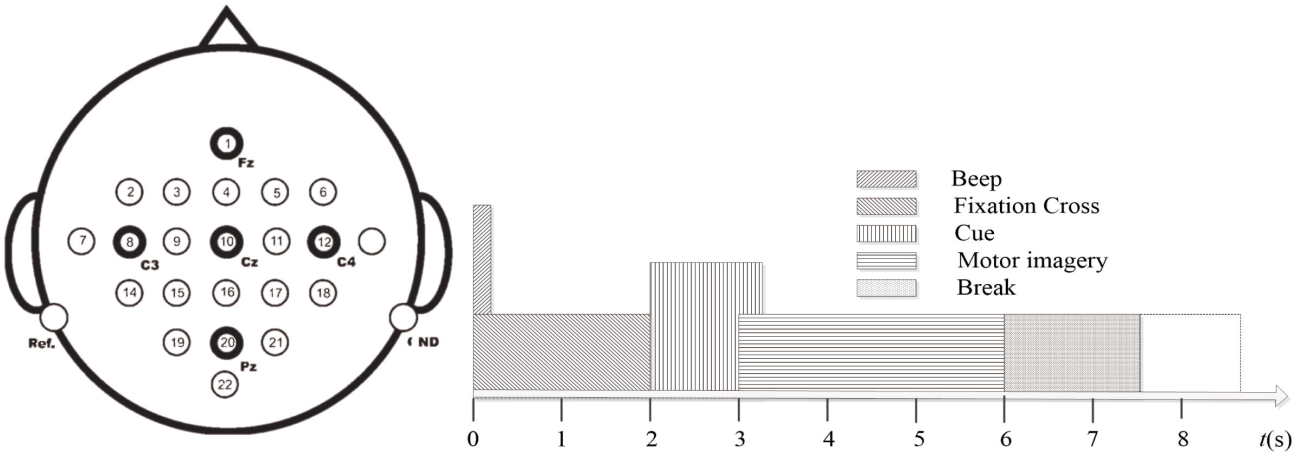

Fig. 1. Electrode montage corresponding to the international 10–20 system (left) and procession for EEG data collection (right).

The rationale for adopting MIC-TEO in this paper is based on the following reasons. First, EEG contains high-frequency information with short interval segments and low-frequency information with long period segments. Teager energy operator (TEO) is very sensitive to frequency and amplitude for signals. Second, the ability to accurately capture position information for brain activity is the key to detecting of the state of motor imagery. The microstate is a feature susceptible to variations of signals. Third, considering that EEG belongs to nonlinear signals, the TEO, as a nonlinear operator, can be used to estimate the TEO of a non-stationary signal, and it is thus well suited for detection.

2. Materials and methods

2.1 EEG records and pre-processing

The EEG data used for this research is from datasets 2a of BCI Competition IV 2008, available in the public domain [31]. This database consists of 9 healthy subjects, and each subject performs four different motor imagery tasks (imagination of movement of the left hand, right hand, both feet and tongue). The locations of the EEG recordings and the timing scheme of the paradigm are illustrated in Fig. 1.

A fixation cross appeared on the black screen at the beginning of a trial (t = 0 s) and was replaced by a cue form of an arrow (pointing to left, right, up and down), which stayed on the screen for 1.25 s at t = 2 s. Then, the subjects were asked to carry out the motor imagery task corresponding to one of the four directions until the fixation cross disappeared from the screen at t = 6 s. Finally, a short break followed when the screen was black. However, the analysis in this paper is focused on the left and right-hand motor imagery. The EEG signals collected were sampled with 250 Hz, and bandpass filtered between 0.5 Hz and 100 Hz. In addition, the alpha band was obtained from the processed EEG data using a bandpass filter. Each of the sessions for motor imagery tasks includes 72 trials.

2.2 Teager energy operator

Based on the hypothesis that an epoch of EEG signals for different motor imagery tasks belongs to nonlinear physiological processes, TEO is a nonlinear operator that can estimate a non-stationary signal's energy [32]. The reasons for proposing this method are as follows: (1) Motor imagery is an activity in different brain regions represented in the EEG signals for different chances. The ability to obtain the location change is very important in analyzing the state of motor imagery. (2) The computation efficiency for feature-based TEO is higher due to it only requiring four points at any given instant. In summary, TEO is suited for analyzing the nonlinear signals, and microstate can also obtain the location information.

MIC-TEO, which is more efficient than the traditional method, can be calculated as (1):

$$\Psi_{eeg}\{s[n]\} = s[n-l]\cdot s[n-m] - s[n-p]\cdot s[n-q] \quad (1)$$

where s[n] the discrete EEG signal and Ψ_{eeg} denotes generalized TEO. It is also noted that 1 + m = p + q.

In this paper, p, l, m, q is represented as 0, 1, 2, and 3 for further analysis in EEG signals.

Considering that the input EEG signal contains white noise, we assume s[n] as EEG signals without noise, so the output of expectation for TEO is as follows:

$$E[0(s(n))] = E\left[s^2(n)\right] - E[s(n-1)s(n+1)] \quad (2)$$

and given the signal with white noise is, $\omega(n)$ the output of expectation for TEO is as (3):

$$\begin{aligned} &x(n) = s(n) + \omega(n) \\ &E[O(x(n))] = E[(s(n)+\omega(n))^2 - (s(n+1)+\omega(n+1)) \\ &(s(n-1)\omega(n-1))] \\ &= E[O(s(n))] + E[O(\omega(n))] + 2E[O(s(n),\omega(n))] \end{aligned} \quad (3)$$

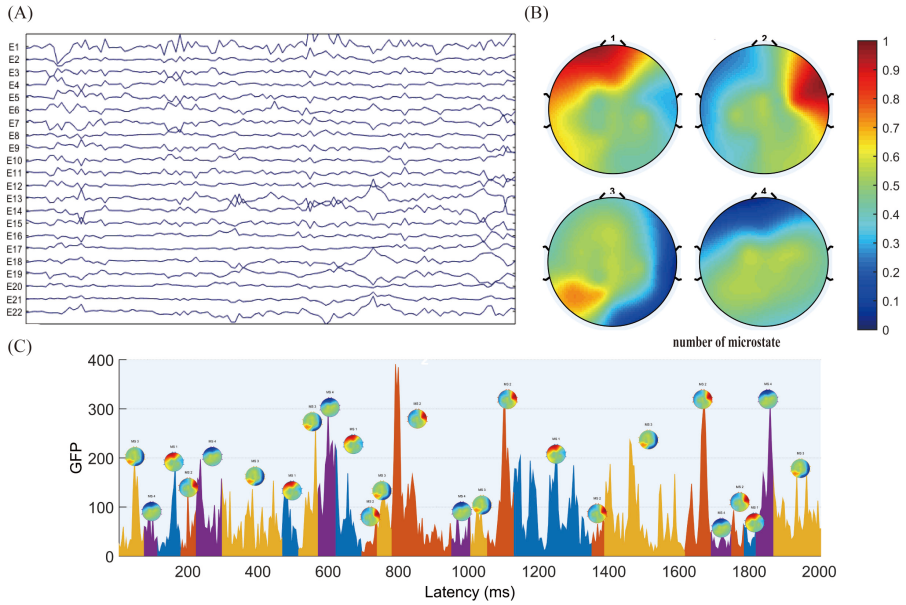

Fig. 2. From EEG signal to microstate. (A) Original potential topography maps were extracted. (B) Original four optimal classes of microstate maps were obtained by a modified spatial cluster analysis method known as the TAAHC. (C) Microstates sequences were obtained by fitting four classes of microstates back to original signals.

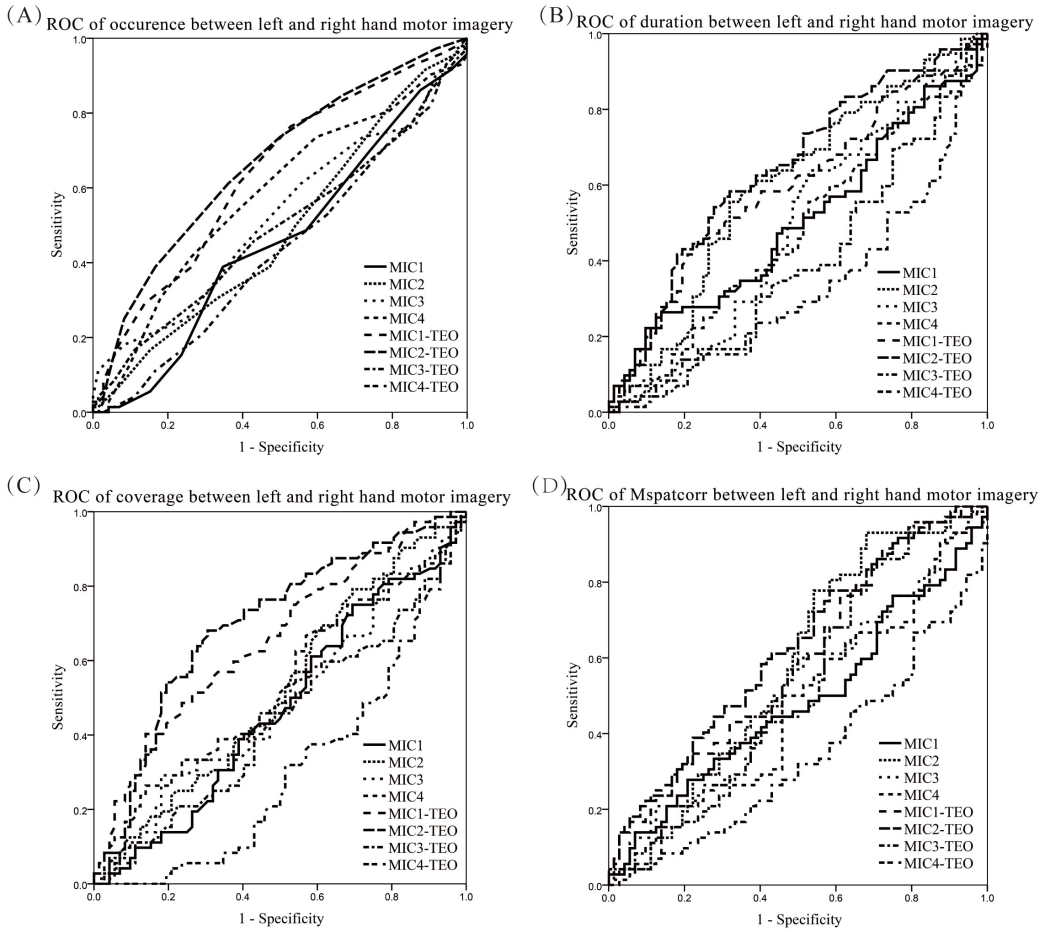

Fig. 3. ROC (The plot of sensitivity vs. (1-specificity) for distinguishing motor imagery tasks) of the parameters (occurrence, duration, coverage and Mspatcorr) from different microstate methods (MIC1 to MIC4 represent microstate one to microstate four based MIC and MIC1-TEO to MIC4-TEO represent microstate one to microstate four based on MIC-TEO) for nine subjects.

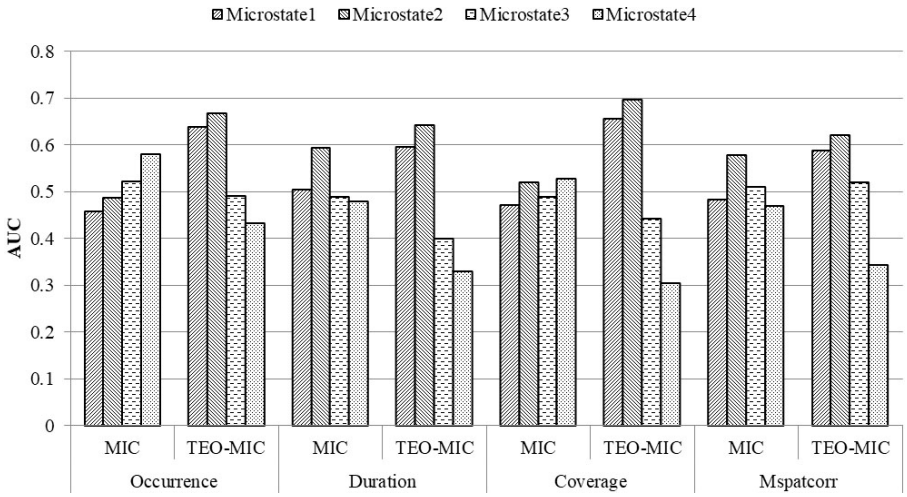

Fig. 4. Areas under the ROC curve with a different method.

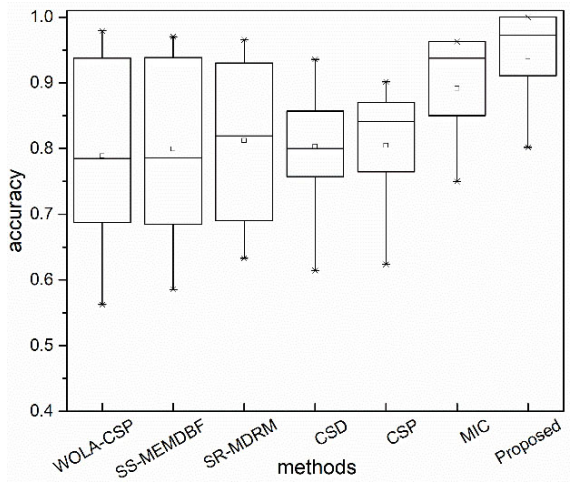

Fig. 5. Average classification performance for different methods in eight different participants. Each box represents the 25–75th percentiles, and the central line is the median value. The thin vertical lines extend to the most extreme data not considered outliners, plotted individually. The performance of different extraction method are compared (CSP represents algorithm of the common spatial pattern, WOLA-CSP represents algorithm of the weighted overlap-add CSP, SS-MEMDBF means the subject specific multivariate empirical mode decomposition based filtering method, SR-MDRM means the minimum distance to Riemannian mean classification based spatially regularized, CSD represents covariate shift-detection and MIC means microstate method) and analyzed to test and verify the effectiveness of the proposed features.

where, $O(s(n), \omega(n)) = s(n)\omega(n) - \omega(n+1)s(n-1) - \omega(n-1)s(n+1)$. Note that $s(n)$ and $\omega(n)$ are zero-mean and mutually independent. Considering that the expectation of $O(s(n), \omega(n))$ is zero, the expectation of $O(x(n))$ is equal to $E[O(s(n))]$ According to the above analysis, TEO can remove the influence of noise with zero-mean.

2.3 EEG Spatio-temporal microstate analysis

We transformed processed EEG signals into a series of momentary potential topographies at GFP peaks. Then the four classes of microstate topographies were obtained by a modified spatial cluster analysis method known as topographical atomize-agglomerate hierarchical clustering (TAAHC), as shown in Fig. 2. For TAAHC, a pre-set number of clusters was avoided. In the beginning, all EEG samples are regarded as an independent cluster center. Next, for each iteration for this algorithm, the worst cluster (defined as the cluster with the lowest sum of correlations between its members and prototype [33]) is chosen and removed. The samples belonging to this worst cluster need to be reassigned to the new cluster they are most similar to. This process continues until only two clusters remain. Note that the number of clustered microstate maps is optimal. Note that the TAAHC ignore the polarity of the topographies. According to the correlation between the templates of four clustered microstate maps, the EEG signal of every single trial was transformed to microstate sequences.

To analyze the differences between left and right motor imagery tasks, four microstate parameters were calculated, as follows: (1) Occurrence- the average number of times per second for one microstate; (2) Duration- the average length of time for one microstate kept stable; (3) Coverage- the percentage of time of activity of a given microstate; (4) Mspatcorr: the mean spatial correlation between a microstate and their assigned EEG trials.

2.4 Cross-validation and statistical analysis

The open-source library (Microstate EEGlab toolbox) provides EEG pre-processing and analysis routines implemented in MATLAB (Version R2014a, Mathworks), and some results were obtained using the Statistical Program for the Social Sciences (SPSS) (IBM SPSS Statistics 22). To evaluate the statistical significance of the MIC-TEO, the paired *t*-test was used as the evaluation criteria to establish a significant difference between two motor imagery tasks. The level

Table 1. Analysis of significance test of 9 subjects for different microstate parameters.

Features	Microstate	Left hand imagery		Right hand immagery		Statistical values	
		Mean	std	mean	std	t	P
Occurence	1	2.68	0.81	2.3	0.81	2.827	**0.005**
	2	2.98	0.75	2.52	0.74	3.61	**0**
	3	3.11	0.89	3.11	0.68	0	1
	4	3.56	0.76	3.76	0.75	−1.606	0.111
Duration	1	73.23	19.45	68.06	17.67	1.669	0.097
	2	79.16	18.43	71.51	20.15	2.377	**0.019**
	3	78.37	16.35	83.74	17.45	−0.902	0.059
	4	91.94	24.62	106.79	28.19	−3.366	**0.001**
Coverage	1	0.2	0.07	0.15	0.06	3.375	**0.001**
	2	0.24	0.07	0.18	0.08	3.679	**0**
	3	0.24	0.08	0.26	0.07	−1.192	0.235
	4	0.32	0.09	0.4	0.11	−4.405	**0**
MspatCorr	1	0.57	0.06	0.54	0.05	2.371	**0.019**
	2	0.54	0.04	0.51	0.05	2.891	**0.004**
	3	0.51	0.03	0.5	0.03	0.799	0.426
	4	0.49	0.03	0.51	0.02	−3.336	**0.001**

The mean and std of the microstate parameters for two motor imagery tasks and tests for statistic test. Bold values indicated $P < 0.05$.

of significance was set at $P < 0.05$. To estimate the performance of the proposed method, 10-fold cross-validation was performed over the training data.

3. Results and discussion

For illustration, two motor imagery task (each subject has 72 for the left hand and 72 for the right hand), as well as mean and standard deviation (std) of microstate parameters (occurrence, duration, coverage, MspatCorr), were conducted to assess the statistical differences between either the two independent variables or their interaction. The results are shown in Table 1. One can observe that microstate one and microstate 2 showed significant differences of four microstate parameters ($P < 0.05$), except for the duration of microstate 1.

As shown in Table 1, compared to the left, microstate 1 and 2 were significantly higher for the left (mean 2.68 times for left and 2.3 times for right for microstate 1). For microstate 2, the situation showed a similar trend with a higher mean for the left (2.98 times per second) than the right (2.52 times per second).

Individually, microstate two was observed with a mean value of 79.16 ms for the left-hand imagery, which decreased to 71.51 ms for the right-hand imagery. However, microstate four was the opposite, with a higher mean for the left-hand imagery (91.94 ms) than for the right hand imagery (106.79 ms). There were significant differences for all microstates between left (mean 0.2, 0.24, and 0.32 respectively) and right (mean 0.15, 0.18, and 0.4 respectively) hand imagery, except for microstate three.

For MspatCorr, the values for the left-hand imagery (mean 0.57 and 0.54 respectively) for microstate one and microstate two were higher than those for the right hand imagery (mean 0.54 and 0.51 respectively). However, for the right-hand imagery, the values from microstate four were higher.

Fig. 3 displays the receiver operating characteristic (ROC) with different parameters based on different methods used in our analysis. Fig. 3 shows that the line in the upper left provides better performance to discriminate between different motor imagery tasks. The area under the curve (AUC) of 1 indicates a perfect classification performance, and the AUC output from SPSS is shown in Fig. 4. Compared with traditional microstate methods, we conclude that the AUC of MIC-TEO is significantly better than MIC method for microstate one and microstate two. However, the AUC of MIC is better or equal to the MIC-TEO method for microstate three and microstate four.

According to the analyses for the differences in microstate parameters, specific features were used to classify the two motor imagery tasks. These selected microstate parameters were: occurrence, duration, coverage, MspatCorr of microstate class 1 and class 2 except for the Duration of microstate class 1, and Duration, MspatCorr of microstate class 4, were used as features for further analysis.

The performances of the proposed methods were also compared with those of previous researchers who had used several state-of-the-art methods using the same database, which is shown in Fig. 5. Note that 90% of samples were selected as a training dataset, and the rest of the samples are used for testing. For all subjects, the mean classification accuracies obtained were: [WOLA-CSP] 78.86% ± 15.07% [SS-MEMDBF] 79.93% ± 14.99% [SR-MDRM] 81.22% ± 13.19% [CSD] 80.32% ± 10.25% [CSP] 80.44% ± 9.53%, [MIC] 89.17% ± 8.1% and [Proposed] 93.93% ± 7.36%. As shown in Fig. 5, the proposed method improved the

mean classification accuracy by 15.07%, 14%, 12.71%, 13.61%, 13.49% and 4.75% in comparison with WOLA-CSP, SS-MEMDBF, SR-MDRM, CSD, CSP and MIC, respectively, which is consistent with the literature [34–39]. Hence, it is clear that the proposed method was more efficient, particularly regarding accuracy and stability.

4. Conclusions

In this paper, we presented a modified algorithm for analyzing EEGs for different motor imagery tasks. The proposed MIC-TEO methods combined the TEO and the MIC methods. The results demonstrated that the proposed algorithm is satisfactory with demonstrated good performance according to ANOVA tests carried out. Thus, it is effective for distinguishing between different motor imagery tasks.

The microstate parameters-occurrence, duration and coverage, as well as Mspatcorr of the microstate sequences obtained were shown significant differences. It demonstrates that the microstate parameters obtained from MIC-TEO of different motor imagery were effective.

The support vector machine classifier was utilized to classify these tasks based on differences in microstate parameters between the motor imagery tasks. The results indicated that the proposed method could be used to extract features. Moreover, it was verified that these features could significantly improve the performance.

Author contributions

YL analyzed the data, wrote and revised this paper; MC revised the paper; SS and ZH write some programmers for this paper; MC, SS, and ZH also make some contributions for the figures.

Ethics approval and consent to participate

Not applicable.

Acknowledgment

Thanks to all the peer reviewers for their opinions and suggestions.

Funding

Funding was provided from Doctoral Scientific Research Starting Foundation of Xi'an University of Posts and Telecommunications (205020018) and the Scientific research plan projects of the Shaanxi Education Department (20JK0917).

Conflict of interest

The authors declare no conflict of interest.

References

[1] Pfurtscheller G, Lopes da Silva FH. Event-related EEG/MEG synchronization and desynchronization: basic principles. Clinical Neurophysiology. 1999; 110: 1842–1857.

[2] Tabar YR, Halici U. A novel deep learning approach for classification of EEG motor imagery signals. Journal of Neural Engineering. 2017; 14: 016003.

[3] Hassan M, Wendling F. Electroencephalography source connectivity: aiming for high resolution of brain networks in time and space. IEEE Signal Processing Magazine. 2018; 35: 81–96.

[4] Power JD, Barnes KA, Snyder AZ, Schlaggar BL, Petersen SE. Spurious but systematic correlations in functional connectivity MRI networks arise from subject motion. NeuroImage. 2012; 59: 2142–2154.

[5] Chavez M, Valencia M, Latora V, Martinerie J. Complex networks: new trends for the analysis of brain connectivity. International Journal of Bifurcation and Chaos. 2010; 20: 1677–1686.

[6] Laureys S, Goldman S, Phillips C, Van Bogaert P, Aerts J, Luxen A, *et al*. Impaired effective cortical connectivity in vegetative state: preliminary investigation using PET. NeuroImage. 1999; 9: 377–382.

[7] Omidvarnia A, Azemi G, Boashash B, O'Toole JM, Colditz PB, Vanhatalo S. Measuring time-varying information flow in scalp EEG signals: orthogonalized partial directed coherence. IEEE Transactions on Biomedical Engineering. 2014; 61: 680–693.

[8] Paszkiel S. Analysis and classification of EEG signals for brain-computer interfaces. Studies in Computational Intelligence. Switzerland: Springer Nature. 2020.

[9] Nunez PL, Srinivasan R. A theoretical basis for standing and traveling brain waves measured with human EEG with implications for an integrated consciousness. Clinical Neurophysiology. 2006; 117: 2424–2435.

[10] Zavaglia M, Astolfi L, Babiloni F, Ursino M. The effect of connectivity on EEG rhythms, power spectral density and coherence among coupled neural populations: analysis with a neural mass model. IEEE Transactions on Bio-Medical Engineering. 2008; 55: 69–77.

[11] Zhang H, Yang H, Guan C. Bayesian learning for spatial filtering in an EEG-based brain-computer interface. IEEE Transactions on Neural Networks and Learning Systems. 2013; 24: 1049–1060.

[12] Park C, Looney D, Ur Rehman N, Ahrabian A, Mandic DP. Classification of motor imagery BCI using multivariate empirical mode decomposition. IEEE Transactions on Neural Systems and Rehabilitation Engineering. 2013; 21: 10–22.

[13] Herman P, Prasad G, McGinnity TM, Coyle D. Comparative analysis of spectral approaches to feature extraction for EEG-based motor imagery classification. IEEE Transactions on Neural Systems and Rehabilitation Engineering. 2008; 16: 317–326.

[14] Ramoser H, Müller-Gerking J, Pfurtscheller G. Optimal spatial filtering of single trial EEG during imagined hand movement. IEEE Transactions on Rehabilitation Engineering. 2000; 8: 441–446.

[15] Barachant A, Bonnet S, Congedo M, Jutten C. Multiclass brain-computer interface classification by Riemannian geometry. IEEE Transactions on Bio-Medical Engineering. 2012; 59: 920–928.

[16] Duan X, Xie S, Xie X, Meng Y, Xu Z. Quadcopter flight control using a non-invasive multi-modal brain computer interface. Frontiers in Neurorobotics. 2019; 13: 23.

[17] Li Y, Xie S, Yu Z, Xie X, Duan X, Liu C. Analysis of imagery motor effective networks based on dynamic partial directed coherence. Journal of Biomedical Engineering. 2020; 37: 38–44.

[18] Gonuguntla V, Wang Y, Veluvolu KC. Event-related functional network identification: application to EEG classification. IEEE Journal of Selected Topics in Signal Processing. 2016; 10: 1284–1294.

[19] Xie S, Li Y. EEG effective connectivity networks for an attentive task requiring vigilance based on dynamic partial directed coherence. Journal of Integrative Neuroscience. 2020; 19: 111–118.

[20] Dinov M, Leech R. Modeling uncertainties in EEG microstates: analysis of real and imagined motor movements using probabilistic clustering-driven training of probabilistic neural networks. Frontiers in Human Neuroscience. 2017; 11: 534.

[21] Khanna A, Pascual-Leone A, Michel CM, Farzan F. Microstates in resting-state EEG: current status and future directions. Neuroscience and Biobehavioral Reviews. 2015; 49: 105–113.

[22] Lehmann D, Ozaki H, Pal I. EEG alpha map series: brain micro-states by space-oriented adaptive segmentation. Electroencephalography and Clinical Neurophysiology. 1987; 67: 271–288.
[23] Pascual-Marqui RD, Michel CM, Lehmann D. Segmentation of brain electrical activity into microstates: model estimation and validation. IEEE Transactions on Biomedical Engineering. 1995; 42: 658–665.
[24] Mishra A, Englitz B, Cohen MX. EEG microstates as a continuous phenomenon. NeuroImage. 2020; 208: 116454.
[25] Shaw SB, Dhindsa K, Reilly JP, Becker S. Capturing the forest but missing the trees: microstates inadequate for characterizing shorter-scale EEG dynamics. Neural Computation. 2019; 31: 2177–2211.
[26] Wang H, Dong X, Chen Z, Shi BE. Hybrid gaze/EEG brain computer interface for robot arm control on a pick and place task. Institute of Electrical and Electronics Engineers. 2015; 2015: 1476–1479.
[27] Zhang R, Li Y, Yan Y, Zhang H, Wu S, Yu T, *et al*. Control of a wheelchair in an indoor environment based on a Brain-Computer Interface and automated navigation. IEEE Transactions on Neural Systems and Rehabilitation Engineering. 2016; 24: 128–139.
[28] Sun L, Feng Z, Lu N, Wang B, Zhang W. An advanced bispectrum features for EEG-based motor imagery classification. Expert Systems with Applications. 2019; 131: 9–19.
[29] Michel CM, Koenig T. EEG microstates as a tool for studying the temporal dynamics of whole-brain neuronal networks: a review. NeuroImage. 2018; 180: 577–593.
[30] Wei Y, Ramautar JR, Colombo MA, Te Lindert BHW, Van Someren EJW. EEG microstates indicate heightened somatic awareness in insomnia: toward objective assessment of subjective mental content. Frontiers in Psychiatry. 2018; 9: 395.
[31] Brunner C, Naeem M, Leeb R, Graimann B, Pfurtscheller G. Spatial filtering and selection of optimized components in four class motor imagery EEG data using independent components analysis. Pattern Recognition Letters. 2007; 28: 957–964.
[32] Kamath C. Teager energy based filter-bank cepstra in EEG classification for seizure detection using radial basis function neural network. ISRN Biomedical Engineering. 2013; 2013: 1–9.
[33] Khanna A, Pascual-Leone A, Farzan F. Reliability of resting-state microstate features in electroencephalography. PLoS ONE. 2014; 9: e114163.
[34] Liu W, Liu X, Dai R, Tang X. Exploring differences between left and right hand motor imagery via spatio-temporal EEG microstate. Computer Assisted Surgery. 2017; 22: 258–266.
[35] Amardeep S, Sunil L, Hans G. Reduce calibration time in motor imagery using spatially regularized symmetric positives-definite matrices based classification. Sensors. 2019; 19: 379.
[36] Gaur P, Pachori RB, Wang H, Prasad G. A multi-class EEG-based BCI classification using multivariate empirical mode decomposition based filtering and Riemannian geometry. Expert Systems with Applications. 2018; 95: 201–211.
[37] Majidov I, Whangbo T. Efficient classification of motor imagery electroencephalography signals using deep learning methods. Sensors. 2019; 19: 1736.
[38] Raza H, Cecotti H, Li Y, Prasad G. Adaptive learning with covariate shift-detection for motor imagery-based brain–computer interface. Soft Computing. 2016; 20: 3085–3096.
[39] Belwafi K, Romain O, Gannouni S, Ghaffari F, Djemal R, Ouni B. An embedded implementation based on adaptive filter bank for brain-computer interface systems. Journal of Neuroscience Methods. 2018; 305: 1–16.